

## The production of nanocrystalline Titanium carbide compound via mechanical alloying

Ali Seydi<sup>1</sup>, Sepehr Pourmorad<sup>2</sup>, Kave Arzani<sup>3</sup>

Department of Materials Engineering, Science and Research Branch, Islamic Azad University, Tehran, Iran  
[Ali.seydi1@yahoo.com](mailto:Ali.seydi1@yahoo.com)

**Abstract:** A nanocrystalline/nanoparticle TiC refractory compound has been produced by mechanical alloying (MA) of the elemental powders. The phase evolution and microstructural changes of the powders during mechanical alloying were investigated by means of X-ray diffractometry, field-emission scanning electron microscopy, high-resolution transmission electron microscopy and microhardness measurements. The results showed that after an optimum mechanical alloying time of 15 hours, a TiC refractory compound with the crystallite size of less than 10 nm, the particle size of about 80 nm and the lattice strain of 1.8% was achieved. The obtained TiC refractory compound exhibited high microhardness value of about 708 Hv.

[Ali Seydi, Sepehr Pourmorad, Kave Arzani. **The production of nanocrystalline Titanium carbide compound via mechanical alloying.** *Life Sci J* 2012;9(4):5819-5823] (ISSN:1097-8135). <http://www.lifesciencesite.com>. 867

**Keywords:** Nanocrystalline materials; Nanoparticles; Titanium carbide; Refractory compounds; Mechanical alloying

### 1. Introduction

Titanium carbide (TiC) is thermodynamically stable which has a very high melting point (3100 °C)

and does not decompose or undergo phase transformations in any temperature range of interest<sup>1,2</sup>. It has metallic characteristics (luster and metallic conductivity), extraordinary hardness and toughness, and excellent resistance to wear, abrasion and infusibility. Therefore, TiC has been widely produced for some industrial applications such as hard coating to protect the surface of cutting tools from wear and erosion<sup>3</sup>. Normally, titanium carbide is produced by high-temperature processes such as the displacement reaction of titanium oxide and carbon, direct reaction of elemental Ti and C, and self-propagating high temperature synthesis (SHS)<sup>4</sup>. In most cases, these techniques require expensive furnaces and high temperature which should be higher than the melting point of TiC. Moreover, it is difficult to obtain nano-sized TiC powders by these methods. Mechanical alloying (MA) is a rapidly developing technology capable of producing a variety of materials, such as refractory compounds, metastable solid solutions, amorphous alloys, nanocrystalline materials, etc.<sup>5-7</sup>. In comparison to other fabrication techniques, MA process has the advantage of the final product possessing a nanocrystalline structure with superior properties rather than conventional coarse-grained structure<sup>8-10</sup>. Up to now, several compounds such as WC<sup>11</sup>, AlNi<sup>12</sup>, FeAl<sup>6, 13</sup>, NiTi<sup>14</sup>, TiFe<sup>15</sup>, FeNi<sup>16</sup>, AlRu<sup>17</sup>, CoAl<sup>18</sup>, MoSi<sub>2</sub><sup>8</sup>, Ni<sub>3</sub>Al<sup>9, 19, 20</sup>, NbAl<sub>3</sub><sup>21</sup>, Ni<sub>3</sub>Fe<sup>16, 22</sup> and Ni<sub>2</sub>AlTi<sup>23</sup> have been fabricated by mechanical alloying. This study aims to investigate the feasibility of producing simultaneous nanocrystalline and nanoparticle TiC refractory powder via mechanical

alloying process. Phase transformation and structural and morphological evolutions occurring during the mechanical alloying process have also been investigated.

### 2. Experimental procedure

In this investigation, Ti (99.8% purity) and graphite as a source of carbon (99% purity) powders were used as starting materials. Both Ti and C powders had an irregular shape with particle size of less than 10 μm. Mechanical alloying was performed for different milling times using a high energy planetary ball mill machine (Retsch PM400). The milling media consisted of 15 balls with the diameter of 20 mm confined in a 500 ml bowl. Both the ball and the bowl materials were hardened chromium steels. In all MA runs, the ball-to-powder weight ratio was 10:1 and the bowl rotation speed was approximately 350 rpm. In all experimental operations, Ti and C powders in 1:1 molar ratio (Ti<sub>50</sub>C<sub>50</sub>) were mixed together and then milled in argon atmosphere at the room temperature. Stearic acid (CH<sub>3</sub>(CH<sub>2</sub>)<sub>16</sub>COOH) in the quantity of 3 wt.% was utilized as Process-Control Agent (PCA) material to avoid sticking of the powders to the vial and balls. Small amounts of the powders were taken out at selected times as samples for the structural analysis. Samples structures were characterized by a Philips X'PERT MPD X-ray diffractometer with CuK<sub>α</sub> radiation (k = 0.1542 nm). The crystallite size and internal strain of the samples was calculated from the XRD patterns applying the Williamson-Hall method<sup>24</sup>.

$$\beta \cos \theta = \frac{K\lambda}{d} + 2A\varepsilon \sin \theta \quad (1)$$

where  $\theta$  is the Bragg diffraction angle,  $d$  is the crystallite size,  $\epsilon$  is the average internal strain,  $\lambda$  is the wavelength of the radiation used,  $\beta$  is the diffraction peak width at half maximum intensity,  $k$  is the Scherrer constant (0.91) and  $A$  is a coefficient which depends on the distribution of strain being near to unity for the dislocations. The average internal strain can be estimated from the linear slope of  $\beta \cos \theta$  versus  $\sin \theta$ , and the average crystallite size

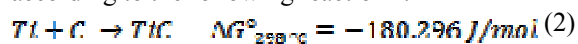
can be estimated from the intersection of this line at  $\sin \theta = 0$ . The microstructures of the powders were

characterized by field-emission scanning electron microscopy (FESEM) (Philips XL30) and high-resolution transmission electron microscopy (HRTEM) (JEOL JEM2100). The microhardness values of the powder particles were determined using a Vickers indenter (Leitz Wetzlar microhardness tester) at the load of 50 g and dwell time of 10 s. For the microhardness measurements, small amounts of powder particles were mounted and their cross-sections were prepared by conventional metallographic techniques. Ten indentations were then performed on each sample to obtain its average microhardness value.

### 3. Results and discussion

#### 3.1. Structural evolution

The Ti-C phase diagram is depicted in Fig. 1. As is seen, the reaction of Ti and C in solid state (with distinct composition in the figure) can take place according to the following reaction<sup>25</sup>:



The negative free energy change of reaction (2) suggests that this reaction can thermodynamically occur during the room temperature mechanical alloying of elemental Ti and C powder mixture, leading to the formation of the TiC refractory compound. Furthermore, it is generally believed that the ball milling process can effectively facilitate the diffusion process by providing high diffusivity paths like dislocation lines and grain boundaries and thus accelerate the Ti-C reaction<sup>12,26</sup>. Therefore, it would be possible to produce TiC compound directly by the MA of the elemental constituent powders. Fig. 2 shows the XRD patterns of Ti-C powder mixture prior to the milling and after different milling times. According to the XRD patterns of the as-received powder, the

diffraction peaks of the pure crystalline Ti and C are evident. In the first 5 hours of the milling process, only the broadening of the Ti and C peaks and a remarkable decrease in their intensities are observed and no TiC peak can be detected. The absence of any shifts in the positions of Ti and C peaks leads to the conclusion that no reciprocal solid solution has been formed. The continuation of the milling for another 5 hours leads to the disappearance of the most individual Ti and C peaks and subsequently appearance of TiC peaks. The transformation of elemental Ti and C powder mixture to the TiC refractory phase is completed after 15 hours of ball milling. The continuation of the milling process for an extra 5 hours brings no further structural changes in the powder. It, however, decreases the intensity of TiC peaks and increases their width as a result of crystallite refinement and lattice strain enhancement<sup>8,12</sup>. Up to date, two kinds of reaction mechanisms have been accepted in MA<sup>2,27</sup>: (1) The colliding balls undergo severe plastic deformation, causing the flattened particles contact with clean surface, and alloys form through gradual diffusion of thin layers, which is called the gradual diffusion reaction (GDR); (2) The alloys form through a reaction taking place within a short period with the liberation of large heat after certain milling time, which is called self-sustained reaction during mechanical alloying, and it is suggested that mechanical impact plays an important role in igniting the reaction. So, the reaction mechanism is usually named mechanically induced self-propagating reaction (MSR). The reaction mechanism of Ti-C system is GDR<sup>1,25</sup>. It has been extensively reported that during GDR mechanism, initial powder particles (such as Ti and C) suffer from very strong high energy impacts attributed to collisions between balls themselves and container wall. These strong impacts will cause large amounts of microstructural and structural defects into the milled powder particles. The presence of such defect structure enhances the diffusivity of solute elements into the matrix. Furthermore, the refined microstructural features shorten the diffusion paths<sup>27,28</sup>. The slight rise in temperature during the milling process also helps diffusion<sup>26,29</sup>. Therefore, the diffusion of C atoms in some of the Ti defects reduces the stress induced by MA. In other words, the solution of C in the Ti lattice compensates the stress which is stored in the Ti lattice due to the defects induced by mechanical alloying. Considering the above results, it seems that 15 hours is an optimum milling time for the production of TiC refractory compound via mechanical alloying process. This is in agreement with previously reported results<sup>10,12,19-21,30-32</sup> implying that it is possible to synthesize refractory compounds directly by mechanical alloying of the elemental constituent powders.

Fig. 3 schematically shows the formation process of nanocrystalline TiC by MA of Ti and C powders. At the initial stage of milling, the carbon powders are easier to be crushed into finer particles, while the large Ti particles are inclined to be plastic deformed and fragmented (Fig. 3(a)). At this stage, no TiC can be detected in the as-milled powders. With increasing milling time, the size of the carbon powders continuously decreases. Fine carbon particles are entrapped between the Ti flakes and the particles are brought into intimate contact (Fig. 3(b)). The intimate contact may lead to the formation of a Ti solid solution Ti(C). The Ti(C) particles are gradually refined during the milling process. The refining of the particles increases the contact area and activities of the reactants. With the milling proceeding, internal stress, and stored energy increase gradually, and when the stress and energy reach a certain degree, the transformation from Ti(C) to TiC will occur<sup>6,27</sup>. In this process, the transformation is believed to depend on atomic diffusion, especially the diffusion of carbon atoms<sup>1</sup>. Furthermore, ball milling will induce a severe internal strain, heavy defects and large volume fraction of grain boundaries, providing an excess short-circuit diffusion pathways and enhancing the reaction rate. A little amount of TiC firstly forms on the surface of the Ti particles (Fig. 3(c)). In addition, the heat generated from the formation of initial TiC raises the temperature in the milling vial, which will accelerate the diffusivity of atoms, especially the C atoms<sup>24,31</sup>. Finally, the as-milled products are fully composed of nanocrystalline TiC and most of TiC nanocrystals tend to agglomerate (Fig. 3(d)).

The crystallite size and internal strain of TiC refractory compound are estimated from the broadening of XRD peaks using Williamson-Hall method. In this method, both of broadening contributions, due to the strain and crystallite size, are taken into account. Fig. 4 plots the TiC crystallite size and internal strain as a function of milling time. Upon ball milling, the TiC refractory compound is readily reached to a nanocrystalline structure. It is important to note that the MA treatment is an effective procedure to reduce the average size domain to nanocrystalline scale in a relatively short time. After 15 hours of milling, the TiC crystallite size and internal strain reaches to 7.5 nm and 1.8%, respectively. As can be observed in Fig. 4, the crystallite size has been sharply decreased at the initial stages of the milling process while it follows a slightly decreasing trend at longer milling times. This phenomenon has also been reported by many researchers<sup>8, 10, 19</sup>. Ball milling is characterized by severe plastic deformation of powder particles under extremely high strain rates resulting in the generation of high density of lattice defects which are primarily dislocations. The progressive

accumulation and interaction of dislocations lead to the refinement of crystallite size as well as increase of the lattice strain<sup>20,21,26</sup>. Fig. 5 illustrates the HRTEM bright field image of the powders collected after 15 hours of milling. The crystallite size of the TiC refractory compound is less than 10 nm, which is in accordance with that calculated by the Williamson-Hall method (see Fig. 4).

### 3.2. Microstructural observations

The FESEM images of the starting material and milled powder for 10 and 15 h are shown in Fig. 6. Changes in particle shapes and sizes caused by MA process are obvious. The TiC nanoparticles are slightly agglomerated. This could be related to high surface energy of nanosized particles. As can be seen from the morphologies of the powders after 15 hours of milling (Fig. 6(d)), the average size of the TiC particles is reduced to 80 nm. When MA is applied, the TiC particles undergo very strong high energy impacts and fractures resulted from collisions during process. Fragments generated by these impacts may continue to reduce the particle size in the absence of strong agglomerating forces<sup>12</sup>. On the other hand, the TiC is a brittle compound. Hence, the fragmentation of this fragile compound is another reason for the observed decrease in the powder particle size and less agglomeration.

### 3.3. Microhardness

Fig. 7 plots the average microhardness values of powder particles at different MA times. In the early stages of milling, the microhardness values increase due to the formation of fine crystalline grains and high density of defects in the powder<sup>19, 27, 31</sup>. For the MA times between 10 to 15 hours, a considerable increase in hardness value of powder particles is observed, which is attributed to the formation of TiC phase. This is in agreement with the XRD results. After complete formation of TiC refractory compound, increasing the MA time from 15 to 20 hours causes the hardness value to increase with a much lower rate mainly due to the decrease in the crystallite size of the TiC phase. It is worth noting that the TiC refractory compound obtained after 20 hours of milling exhibited high microhardness value of about 708 Hv.

As a result of this investigation, in contrast with other similar manufacturing processes and technologies, working at high temperatures or complex reaction conditions, mechanical alloying process could be a very efficient, practically simple and low-cost process for synthesis of pure nanocrystalline/nanoparticle TiC refractory powder with high microhardness value. Using such a process to commercially produce nanocrystalline/nanoparticle TiC has the potential for significant energy and capital

expenditure savings as compared to existing high-temperature production processes currently used to produce TiC.

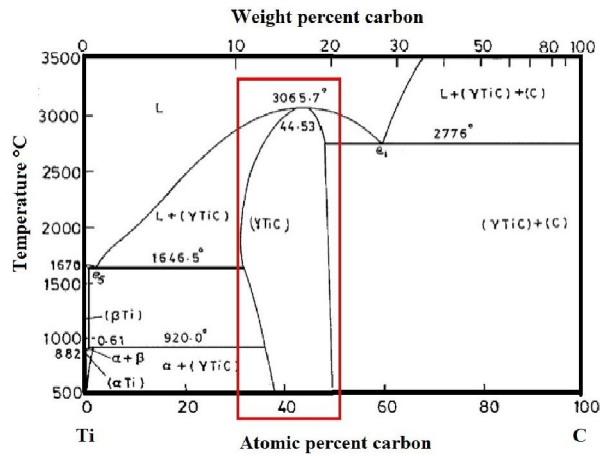


Fig. 1. The Ti-C phase diagram.

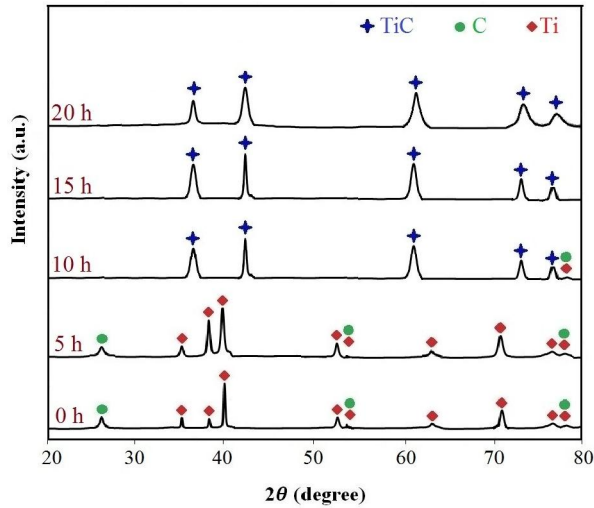


Fig. 2. The XRD patterns of Ti-C powder mixture milled for different times.

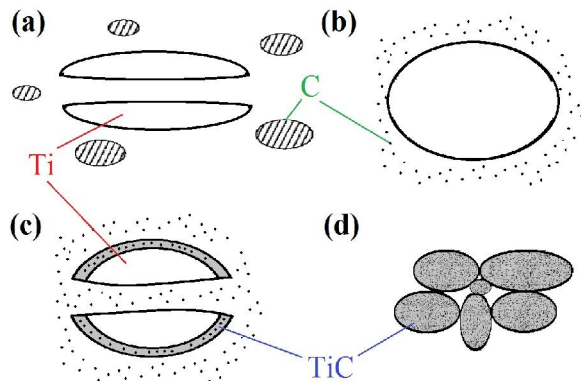


Fig. 3. A schematic showing the reaction progress of Ti and C powders during MA process.

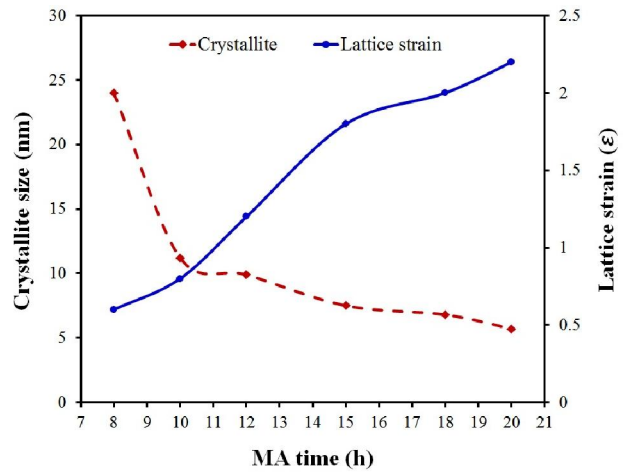


Fig. 4. The variations of the crystallite size and lattice strain of TiC powder at various MA times.

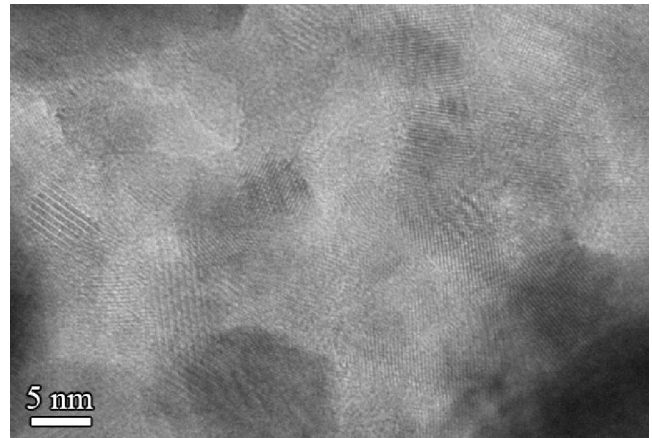


Fig. 5. The high-resolution TEM image of the TiC refractory compound prepared by 15 hours of MA.

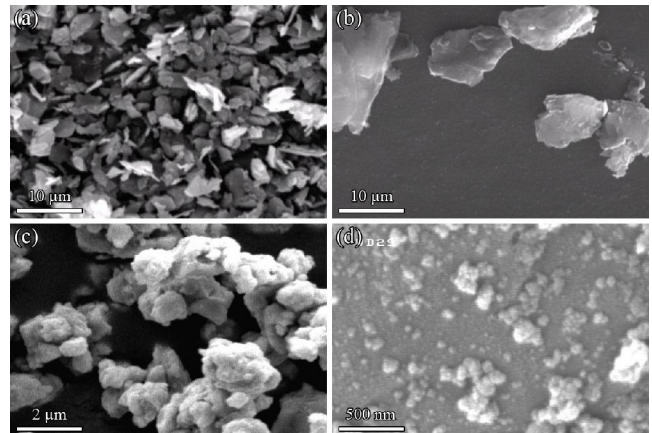


Fig. 6. Typical FESEM images of powders: (a) Ti, (b) C, (c) TiC milled for 10 h and (d) TiC milled for 15 h.

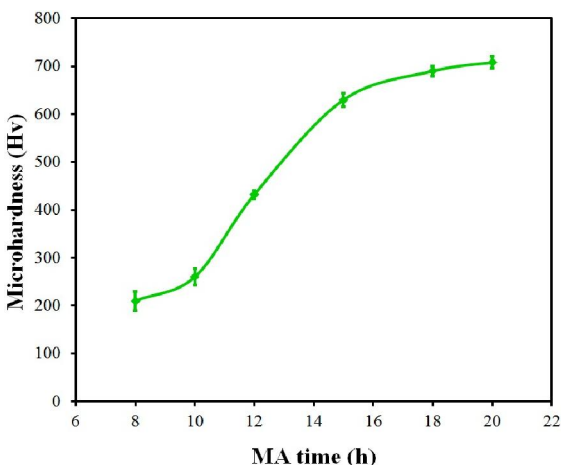


Fig. 7. The microhardness values of powder particles as a function of MA time.

#### 4. Conclusions

Mechanical alloying of  $Ti_{50}C_{50}$  powders led to the gradual formation of nanocrystalline/nanoparticle TiC refractory powder. Results indicated that 15 hours of milling was the optimum time for producing the TiC refractory compound via the mechanical alloying process. After 15 hours of mechanical alloying, a TiC refractory compound was obtained with the crystallite size of less than 10 nm, the particle size of about 80 nm and the lattice strain of 1.8%. The achieved TiC refractory compound exhibited a high microhardness value of about 708 HV.

#### References:

1. B. G. Park, S. H. Ko, and Y. H. Park, *Funtai Oyobi Fumatsu Yakin/Journal of the Japan Society of Powder and Powder Metallurgy*, 2000, **47**(10), 1080-1084.
2. E. S. Tschernikova, I. I. Timofeeva, I. V. Uvarova, A. I. Bykov, V. V. Skorokhod, and V. P. Smimov, *Poroshkovaya Metallurgiya*, 1998(5-6), 32-38.
3. S. H. Ko, B. G. Park, H. Hashimoto, T. Abe, and Y. H. Park, *Mater. Sci. Eng., A*, 2002, **329-331**, 78-83.
4. S. Azem, M. Nechiche, and K. Taibi, *Combustion auto-propagée (SHS) dans les systèmes Ti-C, Ti-Al-C et Fe-Al*, 2011, **99**(4), 449-456.
5. S. E. Aghili, M. H. Enayati, and F. Karimzadeh, *Mater. Manuf. Processes*, 2012, **27**(4), 467-471.
6. R. Esparza, G. Rosas, J. A. Ascencio, and R. Pérez, *Mater. Manuf. Processes*, 2005, **20**(5), 823-832.
7. M. M. Verdian, *Mater. Manuf. Processes*, 2010, **25**(12), 1437-1439.
8. M. Zakeri, R. Yazdani-Rad, M. H. Enayati, and M. R. Rahimpour, *J. Alloys Compd.*, 2005, **403**(1-2), 258-261.

9. Y. Yu, J. Zhou, J. Chen, H. Zhou, C. Guo, and B. Guo, *J. Alloys Compd.*, 2010, **498**(1), 107-112.
10. M. Nazarian Samani, A. Shokuhfar, A. R. Kamali, and M. Hadi, *J. Alloys Compd.*, 2010, **500**(1), 30-33.
11. M. Razavi, M. R. Rahimpour, and R. Yazdani-Rad, *J. Alloys Compd.*, 2011, **509**(23), 6683-6688.
12. M. H. Enayati, F. Karimzadeh, and S. Z. Anvari, *J. Mater. Process. Technol.*, 2008, **200**(1-3), 312-315.
13. Z. G. Liu, J. T. Guo, L. L. He, and Z. Q. Hu, *Nanostruct. Mater.*, 1994, **4**(7), 787-794.
14. T. Mousavi, F. Karimzadeh, and M. H. Abbasi, *Materials Science and Engineering: A*, 2008, **487**(1-2), 46-51.
15. H. Hotta, M. Abe, T. Kuji, and H. Uchida, *Journal of Alloys and Compounds*, 2007, **439**(1-2), 221-226.
16. S. Azadehranjbar, F. Karimzadeh, and M. H. Enayati, *Int. J. Mod Phys B*, 2011, **25**(7), 1013-1019.
17. S. Demedeiros, F. Machado, R. Zampiere, I. Santos, and A. Paesanojr, *Journal of Non-Crystalline Solids*, 2006, **352**(32-35), 3718-3720.
18. S. N. Hosseini, T. Mousavi, F. Karimzadeh, and M. H. Enayati, *Journal of Materials Science & Technology*, 2011, **27**(7), 601-606.
19. R. Ismail and I. I. Yaacob, *Synthesis and characterization of nanocrystalline Ni3Al intermetallic via mechanical alloying and reaction synthesis*. 2006. p. 1121-1126.
20. M. H. Enayati, Z. Sadeghian, M. Salehi, and A. Saidi, *Mater. Sci. Eng., A*, 2004, **375-377**(1-2 SPEC. ISS.), 809-811.
21. Z. Peng, C. Suryanarayana, and F. H. Froes, *Metallurgical and Materials Transactions A*, 1996, **27**(1), 41-48.
22. I. Chicinaş, V. Pop, O. Isnard, J. M. Le Breton, and J. Juraszek, *J. Alloys Compd.*, 2003, **352**(1-2), 34-40.
23. H.-H. Sheu, L.-C. Hsiung, and J.-R. Sheu, *Journal of Alloys and Compounds*, 2009, **469**(1-2), 483-487.
24. G. K. Williamson and W. H. Hall, *Acta Metall.*, 1953, **1**(1), 22-31.
25. D. R. Gaskell, 2008.
26. E. T. Kubaski, O. M. Cintho, and J. D. T. Capocchi, *Powder Technol.*, 2011, **214**(1), 77-82.
27. C. Suryanarayana, T. Klassen, and E. Ivanov, *Journal of Materials Science*, 2011, **46**(19), 6301-6315.
28. H. Mostaan, F. Karimzadeh, and M. H. Abbasi, *Thermochim. Acta*, 2012, **529**, 36-44.
29. W. Pilarczyk, R. Nowosielski, A. Pilarczyk, and P. Sakiewicz, *Archives of Materials Science and Engineering*, 2011, **47**(1), 19-26.
30. M. Rozmus, M. Blicharski, and S. Dymek, *Journal of Microscopy*, 2006, **224**(1), 58-61.
31. A. J. Heron and G. B. Schaffer, *J. Mater. Synth. Process.*, 1994, **2**(5), 335-340.
32. M. Fukumoto, M. Yamasaki, M. Nie, and T. Yasui, *Yosetsu Gakkai Ronbunshu/Quarterly Journal of the Japan Welding Society*, 2006, **24**(1), 87-92.

12/15/2012